The 2015 World Congress on
Advances in Civil, Environmental, and Materials Research (ACEM15)
Incheon, Korea, August 25-29, 2015

Characteristics of artificial reefs in installation stages

Sol Han[1)], Dongha Kim[1)], Quynh T.N. Le[1)] and *Won-Bae Na[2)]

[1), 2)] *Dept. of Ocean Engineering, Pukyong National University, Busan 609-737, Korea*
[2)] *wna@pknu.ac.kr*

ABSTRACT

Most of artificial reefs (ARs) are installed on the seabed by means of a free fall or certain guided way. Relatively cheaper and smaller artificial reefs are generally installed by a free fall procedure from the water surface while expensive and larger ARs are established on the seabed using wires, cables, divers, and other mechanical ways. In Korea, cube type ARs are the most popular because their durability, inexpensive cost, and others. When these reefs are launched from a barge, their falling behaviors are not well understood. Besides, recently, the partial settlement of the seabed caused by AR installation becomes an issue. To provide the stability of ARs against partial settlement, sliding, and overturning, it is important to understand the initial settlement of ARs during the employment and necessary to figure out the impact energy of ARs when they collide on the seabed. Accordingly, the drag coefficients (pressure drag or form drag) of employing ARs are significant for the calculation of the impact energy. This study presents a procedure in obtaining the pressure drag coefficient, their values, and associated impact energies to the seabed. For the purpose, flow characteristics around these ARs were investigated to calculate the pressure fields and other hydraulic measures. From the flow analyses, it is found that the maximum kinetic energies of the four cube type ARs are 14.43 (C1), 86.89 (C2), 110.31 (C3), and 38.80kJ (C4).

1. INTRODUCTION

Most artificial reefs (ARs) are installed on the seabed by means of a free fall or certain guided way. Relatively cheaper and smaller ARs are generally installed by a free fall procedure from a barge on the water surface while expensive and larger ARs are established on the seabed using wires, cables, divers, and other physical ways. Thanks to modern development of materials, some countries such as Japan, Korea, and China have developed large-scaled artificial reefs; hence, the installation methods have been concerned (Kim *et al.*, 2014a, 2014b). However, although the size of ARs considered is small, the installation procedure is still important because the ARs usually settled down into the seabed owing to its weight and the effect of multiple

[1)] Graduate Students
[2)] Professor

arrangements. This phenomenon was reported by several researchers (Manoukian *et al*. 2011). To obtain the settlement depth, the velocity profile of an AR with respect to water depth is required and accordingly the drag coefficient should be known. This study proposes the procedure with some cases.

In fluid mechanics, drag refers to forces acting on a solid in the direction of the relative fluid flow velocity. Drag forces can be classified into the several categories. The first is called parasitic drag consisting of pressure drag (or form drag), friction drag (or skin friction), and interference drag. The other two are called lift-induced drag and wave drag (aerodynamics) or wave resistance (water wave dynamics). Among them, pressure drag and friction drag are significant in determining the total drag force acting on an underwater body (Hasanloo et al., 2012) such as artificial reefs (ARs). These drags all follow the drag equation

Pressure drag arises because of the form of the solid. This drag is a force resulting from pressure differences across the obstacle in a flow field. For example, in the ocean, pressure drag occurs when currents flow over or around an object. The size and shape of the solid object are the most significant factors determining pressure drag; solids with a larger apparent cross-section have a larger drag coefficient. Pressure drag increases with the square of the velocity with which the object is moving through the fluid, and thus becomes more significant at high speeds. Friction drag arises from friction of the fluid against the 'skin' of the object. This drag is due to the tangential forces that result when a fluid flows over a surface; hence, a rough surface results in more friction drag. Friction drag is directly related to the wetted surface, i.e., the surface area that is in contact with the fluid. Friction drag also increases with the square of the velocity. It should be noted that the drag coefficient for all objects with a sharp edge is essentially independent of the Reynolds number (for $Re \geq 1000$) because of the separation points (Fox et al. 2004). In general, the magnitude of the pressure cannot be determined analytically; hence, experimental or numerical methods are required.

Woo and Na (2014) determined the drag coefficient of 2-ton stock and stockless anchors using the element-based finite volume method (FVM). They only considered pressure drag in the calculations because pressure drag is dominant owing to the shapes of the anchors considered. With a similar method, the drag coefficients of 24 Korean general artificial reefs were obtained by Woo *et al*. (2014). However, in the calculations, the 24 ARs were assumed to be installed on the seabed. Thus, the flow direction is different from the scope in this study, the consideration of free fall of ARs.

2. MATERIALS AND METHODS

ANSYS CFX was used for the numerical modeling (ANSYS-Inc. 2009). It utilizes the finite volume technique, which divides the region of interest into sub-regions and discretizes the governing equations and solves them iteratively over each sub-region. The value of each variable at the nodal points over the domain can then be evaluated. The reliability of this method has been established by a number of reports (Finnegan and Goggins 2012, Gylys *et al*. 2012, Kim *et al*. 2012, Versteeg and Malalasekera 1995, Zakeri 2009).

Fig. 1 shows the 3D models of four cube-type ARs considered in the study. The dimensions of the ARs are 2×2×2m^3 (C1), 3×3×3m^3 (C2), 3×3×3m^3 (C3), 3×3×3.5m^3 (C4), respectively. The difference between C2 and C3 is the presence of internal steel box in C3. Fig. 2 shows the water field (hemisphere with diameter of 15m) described by an inlet and outlet. In the figure, the upper plane indicates an outlet and lower surface denotes an inlet. From the inlet, the water flow flows in to the domain with a constant speed (here, 2m/s) and the water flow passes by the target AR (not shown in the figure) located in the center of the domain, and finally the water flow passed by flows out through the outlet by assigning null pressure. The mesh sizes were selected as follows: 0.04m near artificial reefs and 0.2m (the maximum) far from ARs. This domain is very close to the one used by Woo and Na (2004) because the major purpose of the flow analysis is to get the drag coefficients of free falling bodies. Meanwhile, Woo *et al*. (2014) used a parallepiped for the domain to obtain the drag coefficients of installed ARs on the seabed. Through the numerical analyses, the following hypotheses were made. First, the water is incompressible, viscous, and Newtonian. Second, the water temperature is 25℃. Third, the turbulence model is k-ε model. Fourth, the design water velocity is 2m/s.

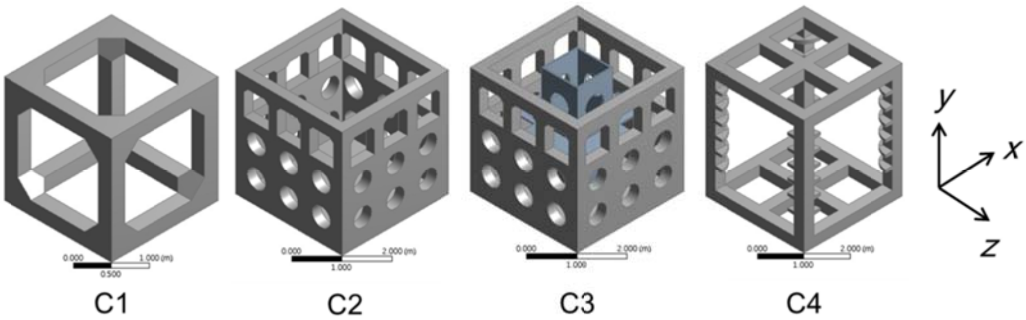

Fig. 1 3D models of box type ARs

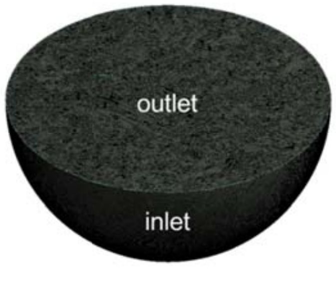

Fig. 2 AR1 (cube type AR) used in the study

3. RESULTS

Table 1 shows the drag (form drag) coefficients of the ARs. It is found that C4 has the largest drag coefficient (1.74), followed by C1, C3, and C4. Fig. 3 shows the velocity vs time curve for each AR (C1, C2, C3, or C4). As shown in the figure and Table 1, it is found that the terminal velocities (the maximum velocities) were 3.87 (C1), 4.27 (C2), 4.13 (C3), and 3.71m/s (C4). Thus, C2 has the highest terminal velocities. The arriving times to the terminal velocities were 2.80 (C1), 3.30 (C2), 2.30 (C3), and 2.30 s (C4). This indicates that C3 and C4 reach to the terminal velocities in the fastest way. Fig. 4 shows the velocity vs distance curve for each AR indicating the critical depths of 12.84 (C1), 14.80 (C2), 12.78 (C3), and 10.91 m (C4). Here, the critical depths correspond to the water depths that the ARs reach to the terminal velocity. These results are also summarized in Table 1.

Table 1 Drag coefficients and other measures

AR	Drag coefficient	Terminal velocity (m/s)	Critical depth (m)	Reduced Mass (kg)	Kinetic energy (kJ)
C1	1.35	3.87	12.84	1929.87	14.43
C2	1.14	4.27	14.80	9544.90	86.89
C3	1.22	4.13	12.78	12915.10	110.31
C4	1.74	3.71	10.91	5623.10	38.80

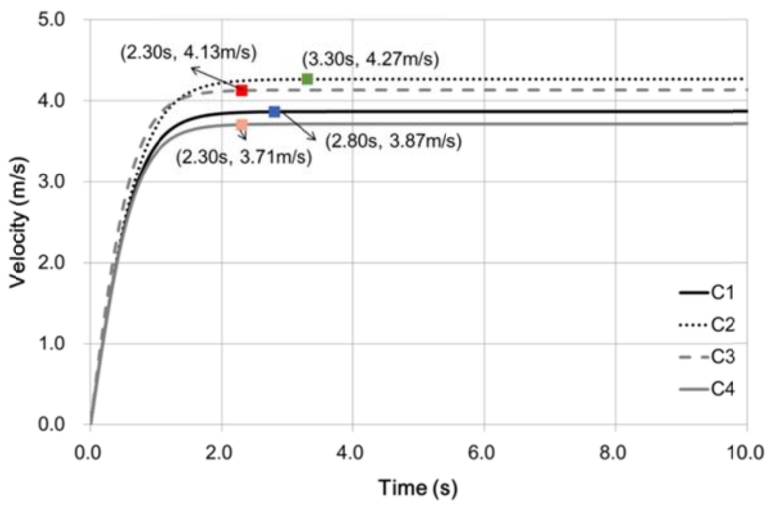

Fig. 3 Velocity vs time

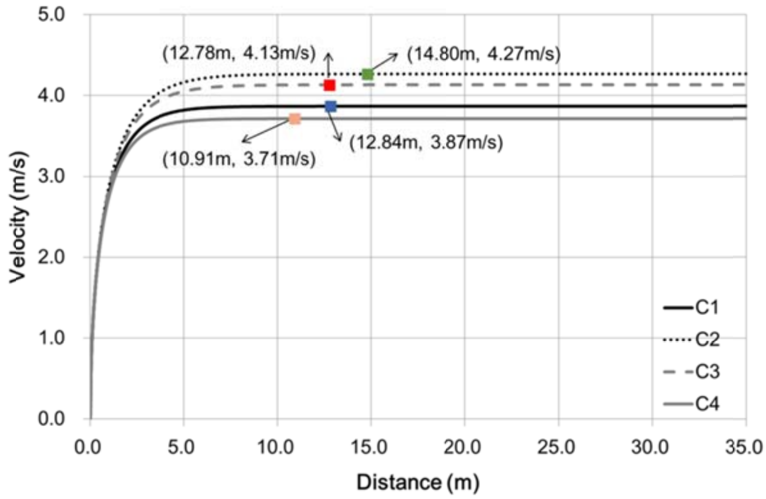

Fig. 4 Velocity vs distance

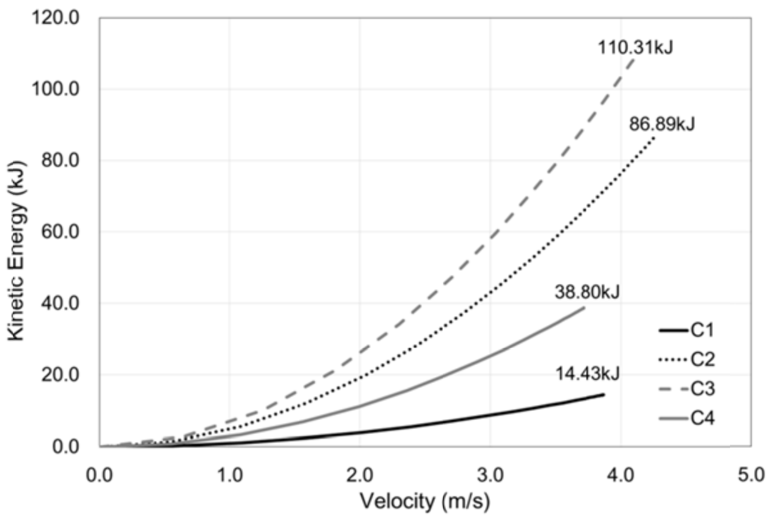

Fig. 5 Kinetic energy vs velocity, the final values show the maximum energies corresponding to the terminal velocities

Fig. 5 shows the kinetic energy vs velocity curve for each AR. Once each AR reaches to the terminal velocity, the kinetic energy becomes maximized such as 14.43 (C1), 86.69 (C2), 110.3 (C3), and 38.80 kJ (C4). The reason why C3 has the largest kinetic energy is simple because of its relatively higher terminal velocity and largest reduced mass among the four. Here, the reduced mass stands for the mass considering buoyancy effect and accordingly the mass is smaller than the original body mass.

Fig. 6 shows the kinetic energy vs distance curve for each AR. This curve indicates that C4 reaches to the maximum kinetic energy at the depth of 13.51m, and other cases reach to the maximum kinetic energy at 13.61 (C1), 19.03 (C3), and 20.35 m (C2). In other words, if those ARs are installed more than 21m water depth, then all of the ARs exceed the critical depths and accordingly hit the seabed with the maximum kinetic energies. Once obtained the maximum kinetic energies, the next step should be simulating the impact of the ARs to the seabed. To do so, it is natural to adopt a reasonable material model of seabed soils and carry out collision analysis. Then, we can estimate the settlement during AR collision.

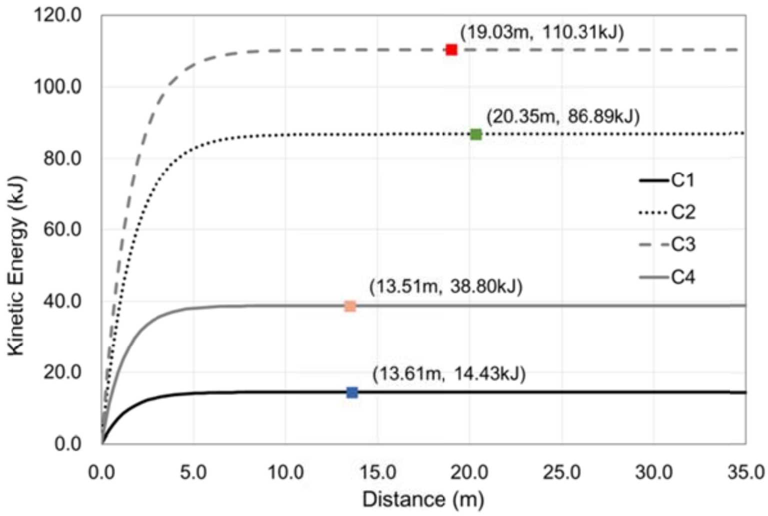

Fig. 6 Kinetic energy vs distance, the values indicate the critical water depths (m) and corresponding kinetic energy (kJ)

4. CONCLUSIONS

Four cube type artificial reefs were investigated to obtain their drag coefficients, terminal velocities, and kinetic energies. For the purpose, flow analyses, implemented by the element-based finite volume method, were conducted. From the analysis results, it is found that the largest drag coefficient occurs to C4 (1.74), followed by C1 (1.35), C3 (1.22), and C2 (1.14). The corresponding terminal velocities are 3.71 (C4), 3.87 (C1), 4.13 (C3), and 4.27m/s (C2). Accordingly, the maximum kinetic energies are 38.80 (C4), 14.43 (C1), 110.31 (C3), and 86.89kJ (C2) due to their reduced masses and terminal velocities.

REFERENCES

ANSYS-Inc. (2009), *ANSYS CFX*, Release 12.1.

Finnegan, W. and Goggins, J. (2012), "Numerical simulation of linear water waves and wave-structure interaction," *Ocean Engineering*, **43**, 23–31.

Fox, W.R., McDonald, A.T. and Pritchard, P.J. (2004), *Introduction to Fluid Mechanics*, Wiley.

Gylys, J., Paukštaitis, L. and Skvorčinskienė, R. (2012), "Numerical investigation of the drag force reduction induced by the tow-phase flow generating on the solid body surface," *International Journal of Heat and Mass Transfer*, **55**, 7645–7650.

Hasanloo, D., Pang, H. and Yu, G. (2012), "On the estimation of the falling velocity and drag coefficient of torpedo anchor during acceleration," *Ocean Engineering*, **42**, 135–146.

Kim, K.P., Ahmed, M.R. and Lee, Y.H. (2012), "Efficiency improvement of a tidal current turbine utilizing a larger area of channel," *Renewable Energy*, **48**, 557–564.

Kim, D., Woo, J., Yoon, H.S. and Na, W.B. (2014a), "Wake lengths and structural responses of Korean general artificial reefs," *Ocean Engineering*, **92**, 83-91.

Kim, D., Woo, J., Na, W.B. and Yoon, H.S. (2014b), "Flow and structural response characteristics of a box-type artificial Reef," *Journal of Korean Society of Coastal and Ocean Engineers*, **26**(3), 113-119.

Manoukian, S., Fabi, G. and Naar, D. (2011), "Multibeam investigation of an artificial reef settlement in the Adriatic sea (Italy) 33 years after its deployment," *Brazilian Journal of Oceanography*, **59**, 145-153.

Versteeg, H.K. and Malalasekera, W. (1995), *An Introduction to Computational Fluid Dynamics: The Finite Element Volume Method*, Longman Group, Ltd.

Woo, J. and Na, W.B. (2014), "Drag coefficients of stock and stockless anchors," *Marine Technology Society Journal*, **48**(3), 138-145.

Woo, J., Kim, D., Yoon, H.S. and Na, W.B. (2014), "Characterizing Korean general artificial reefs by drag coefficients," *Ocean Engineering*, **82**, 105-114.

Zakeri, A. (2009), "Submarine debris flow impact on suspended (free-span) pipelines: Normal and longitudinal drag forces," *Ocean Engineering*, **36**, 489–499.